Accepted Manuscript

Title: Pharmacokinetics and metabolism of GW9508 in rat by liquid chromatography/electrospray ionization tandem mass spectrometry

Authors: Yu Li, Xue Yang, Hui Zhang, Qiuhong Wu

Please cite this article as: Li Y, Yang X, Zhang H, Wu Q, Pharmacokinetics and metabolism of GW9508 in rat by liquid chromatography/electrospray ionization tandem mass spectrometry, *Journal of Pharmaceutical and Biomedical Analysis* (2019), https://doi.org/10.1016/j.jpba.2019.03.040

Pharmacokinetics and metabolism of GW9508 in rat by liquid chromatography/electrospray ionization tandem mass spectrometry

Yu Li [a], Xue Yang [b], Hui Zhang [a], Qiuhong Wu [a*]

[a] Department of Pharmacy, Maternal and Child Health Care Hospital of Zaozhuang, No. 25 East Cultural Road, Zaozhuang 277100, China

[b] Department of Pharmacy, Liaocheng People's Hospital, No. 67 West Dongchang Road, Liaocheng 25200, China

Correspondence

Qiuhong Wu

Department of pharmacy, Maternal and child health care hospital of Zaozhuang, No. 25 East Cultural Road, Zaozhuang 277100, China

Tel: +86-0632-3699056; Fax: +86-0632-3699056

Email:wu_qiuhong@126.com; aoj08@sina.com

Highlights

- An LC/MS/MS method for the quantification of GW9508 in rat plasma
- Pharmacokinetics of GW9508 was investigated
- Oral bioavailability was 54.88%
- Metabolites of GW9508 were characterized by LC-Q-Exactive-Orbitrap-MS
- Hydroxylation and glucuronidation were the primary metabolic pathways

ABSTRACT

In this study, a simple, fast and sensitive LC/MS/MS method was developed and validated for the determination of GW9508 in rat plasma. The sample was precipitated with acetonitrile and subsequently separated on ZORBAX Eclipse XDB C_{18} column (50 mm $\times$ 2.1 mm, 5 μm). Mobile phase was composed of 0.1% formic acid in water and acetonitrile with gradient elution, at a flow rate of 0.4 mL/min. The analyte and internal standard were quantitatively monitored with precursor-to-product transitions of m/z 348.2→183.1 and m/z 397.2→260.2, respectively. The linearity of the assay was evident in the range of 1-1000 ng/mL with correlation coefficient more than 0.998. The validation parameters were all within the acceptable limits. The validated method has been successfully applied to the pharmacokinetics study of GW9508 in rat plasma, and our results demonstrated that GW9508 showed low clearance, moderate half-life and ideal bioavailability (54.88%). Furthermore, metabolites stemmed from rat plasma, rat hepatocytes and human hepatocytes were analyzed by an LC-Q-Exactive-Orbitrap-MS assay, resulting in the identification of seven metabolites based on the accurate mass and fragment ions. Acylglucuronide conjugate (M6) was found as the most abundant metabolite in all tested matrices. The metabolic pathways were proposed as hydroxylation and glucuronidation. This study provided an overview of disposition of GW9508, which is highly instructive for better understanding the effectiveness and toxicity of this drug.

Keywords: GW9508, pharmacokinetics, metabolism, rat hepatocytes, human hepatocytes

1. Introduction

Type 2 diabetes mellitus, a metabolic syndrome, is characterized by insufficient insulin secretion, which has been emerging as one of the serious health problems [1, 2], as it can result in cardiovascular complications, renal failure, and other complications [3-5]. Free fatty-acid receptor 1 (FFAR1), known as human GPR40 receptor (GPR40), has been emerging as one of the antidiabetic targets [6-8]. A number of GRP40 agonists have been developed as therapeutical agents for type 2 diabetes mellitus, such as TAK-875 and AMG-837 [9-14]. Although numerous GPR40 agonists were discovered, a majority of these agonists were failed in developmental stage due to the concerns about liver injury [15, 16]. GW9508 is a potent and selective GPR40 agonist with EC_{50} of 7.32 nM, which was developed by GlaxoSmithKline as a therapeutical agent for type 2 diabetes mellitus [17]. GW9508 can regulate insulin sensitivity and glucose homeostasis by activating Atk/GSK-β pathway and reducing fetuin-A levels [18, 19]. It also can inhibit insulin secretion by activating ATP-sensitive potassium channels in rat pancreatic β-cells [20, 21].

Drug metabolism and pharmacokinetics (DMPK) is an integral part in drug discovery and development. In some cases, DMPK property affects a drug's *in vivo* exposure and in turn, the efficacy and toxicity and numerous examples demonstrated that DMPK property is one of the determinants of drug success [22]. From the point view of chemical structure, GW9508 involves a phenylpropanoic acid in the molecule, which is vulnerable to glucuronidation to form acyl glucuronide. In addition, phenylpropanoic acid is also readily subjected to β-oxidation [23]. As far as we know, the detailed DMPK profiles of GW9508 remain unknown. LC/MS has been becoming as an indispensable and reliable tool for DMPK study because of its high sensitivity and selectivity; especially the high

resolution LC/MS can provide the accurate structural information of drugs and their metabolites; in addition, the concept of mass defect filter (MDF) can automatically remove the interfering peaks, which facilitates the characterization of the metabolites [24].

Therefore, the current study aimed at 1) developing and validating an LC/MS/MS assay for the measurement of GW9508 in rat plasma; 2) investigating the pharmacokinetics of GW9508 in rat plasma after oral and intravenous administration; 3) identifying the metabolites from rat plasma, rat hepatocytes and human hepatocytes; and 4) proposing the metabolic pathways of GW9508. This study is the first report on the pharmacokinetics and metabolism of GW9508, which would be helpful in understanding the effectiveness, toxicity and safety.

2. Materials and methods

2.1. Chemicals and reagents

GW9508 (purity: 99.73%) and PF-04620110 (purity: 98.47%, internal standard, IS) were purchased from Selleck Chemicals (Shanghai, China). Cryopreserved male Sprague-Dawley rat hepatocytes (n = 12) were obtained from BD Gentest (Woburn, MA). Cryopreserved male human hepatocytes (n = 10) were supplied by the Research Institute for Liver Diseases (Shanghai) Co., Ltd. (Shanghai, China). HPLC-grade acetonitrile was purchased from Merck (Darmstadt, Germany). Deionized water was prepared by a Milli-Q Water Purification System (Millipore Corp., MA, USA). All other chemicals and reagents were of analytical grade and obtained from Sinopharm Chemical Co. Ltd (Shanghai, China).

2.2. Animals, drug administration and sample collection

Twelve male Sprague-Dawley rats with body weight of 220 ± 20 g were provided by the Animal Experiment Center of Maternal and Child Health Care Hospital of Zaozhuang (Zaozhuang, China).

The rats were kept in an environmentally controlled breeding room (temperature 25 ± 5 ^{o}C, humidity 55-65%) with food and water being freely available. The rats were acclimated to the facilities and the environment for 5 days before experiments. Before experiments the rats were fasted for 12 h but free access to water. The animal experiments were approved by the Review Committee of Animal Care and Use of Maternal and Child Health Care Hospital of Zaozhuang (Zaozhuang, China). GW9508 was prepared in 0.5% DMSO-0.5% carboxymethyl cellulose sodium salt-99% saline for dosing. The solution was stirred at room temperature until use. For oral administration ($n = 6$), GW9508 was given to rat via gavage at a single dose of 1 mg/kg; for intravenous administration ($n = 6$), GW9508 was administered to rat via tail vein at a single dose of 1 mg/kg. The blood samples (∼120 μL) were collected into clean tubes containing EDTA-Na$_2$ at pre-dose, 0.083, 0.25, 0.5, 1, 2, 4, 8, 12, and 24 h post-dose. The blood samples were immediately centrifuged at 4000 rpm for 5 min, and the resulting plasma samples were transferred into clean tubes and then stored at -80 ^{o}C until analysis.

2.3. Plasma sample preparation

To prepare the plasma sample, an aliquot of 50 μL of rat plasma was placed in a 1.5-mL centrifuge tube. An aliquot of 5 μL of IS working solution (400 ng/mL) was spiked followed by adding 250 μL of acetonitrile. After being thoroughly mixed by vortexing, the mixture was then centrifuged at 15000 rpm for 10 min, and the resulting supernatant was transferred into another tube and then blown dry with nitrogen gas. The residue was then re-dissolved with 100 μL of acetonitrile-water solution (*v:v*, 1:9) and 2 μL of the solution was injected into LC/MS/MS system for analysis.

To detect and identify the metabolites present in rat plasma, the plasma samples were pooled according to AUC rule [25, 26]. A total of 0.6 mL of pooled plasma sample was mixed with 2.4 mL of acetonitrile and then the sample was centrifuged at 15000 rpm for 10 min to remove the denatured

protein. The supernatant was dried with nitrogen gas and the residue was re-dissolved with 100 μL of acetonitrile-water solution (*v:v*, 1:9). An aliquot of 2 μL of the supernatant was injected into LC-Q-Exactive-Orbitrap-MS for analysis.

2.4. *In vitro* metabolism

A stock solution of GW9508 (10 mM) was prepared in DMSO and then diluted with 50% acetonitrile solution and Williams' E medium to yield the working solution (50 μM). Cryopreserved hepatocytes (rat and human) were stored in liquid nitrogen before use. Thawing was carried out according to the manufacture's instruction, after which the hepatocytes were suspended in Williams' E medium to yield a cell concentration of 1.25 million cells/mL. The viability, determined using the trypan blue exclusion method, was found to be > 85.8%. Subsequently, an aliquot of 200 μL of hepatocytes suspension was added into 24-well plate followed by adding 50 μL of GW9508 working solution. The organic solvent in the incubation system was < 0.2% (*v/v*). The total incubation volume was 250 μL. The hepatocyte density was 1 million cells/mL and the concentration of GW9508 in incubation system was 10 μM. The incubations were conducted in a humidified CO_2 incubator at 37 °C. Incubations without GW9508 served as blank controls. After incubation for 2 h, the reactions were stopped by adding 1.0 mL of ice-cold acetonitrile. The samples were transferred into tubes and then centrifuged at 15,000 rpm for 10 min. The supernatants were evaporated to dryness under nitrogen gas. Each residue was dissolved in 100 μL of acetonitrile-water solution (*v/v*; 1:9) and an aliquot of 2 μL of each sample was injected into the LC-Q-Exactive- Orbitrap-MS system for analysis.

2.5. Instrumentation and conditions

2.5.1. LC/MS/MS

The LC/MS/MS system was composed of a Thermo Dionex Ultimate 3000 LC system (Thermo

Fisher Scientific, USA) equipped with a binary pump, sample manager and column manager and a TSQ Vantage triple quadrupole tandem mass spectrometer equipped with an electrospray ionization (ESI) interface (Thermo Fisher Scientific, USA) operated in positive ion mode. LC separations were achieved on a ZORBAX Eclipse XDB C_{18} column (Agilent Technologies, 50 mm × 2.1 mm, 5 μm) kept at 35 °C. The mobile phase was made up of water containing 0.1% formic acid (A) and acetonitrile (B) with gradient programs as follows: 10% B at 0-0.2 min, 10-45% B 0.2-0.8 min, 45-90% B at 0.8-1.3 min, 90% B at 1.3-1.6 min, and 10% B at 1.6-2.0 min. The flow rate was maintained at 0.4 mL/min. The auto-sampler was kept at 10 °C. The injection volume was 2 μL.

Source parameters were optimized as follows: spray voltage 3.0 kV, vaporizer temperature 200 °C, capillary temperature 250 °C, sheath gas 40 arb, and auxiliary gas 10 arb. Quantification was performed by using selected reaction monitoring (SRM) mode. The precursor-to-product quantifier transitions were optimized to be m/z 348.2→183.1 and m/z 397.2→260.2 for GW9508 and IS, respectively. The precursor-to-product qualifier transitions were m/z 348.2→288.1 and m/z 397.2→138.0 for GW9508 and IS, respectively. The collision energy was 25 eV for GW9508 and 45 eV for IS. The dwell time was 100 ms for each transition. Data acquisition and processing were accomplished with Xcalibur software (Version 2.3.1, Thermo Fisher Scientific, USA).

2.5.2. LC-Q-Exactive-Orbitrap-MS

For metabolite identification, a Waters ACQUITY H-class LC system (Waters Co., Milford, MA, USA) coupled with Waters ACQUITY BEH C_{18} column (100 × 2.1 mm, 1.7 μm) was employed for LC separation. The column was kept at 35 °C. The mobile phase was composed of 2 mM ammonium acetate solution (A) and acetonitrile containing 0.2% formic acid (B), which was delivered at a flow rate of 0.4 mL/min. The gradient program was set as follows: 0-1 min 10% B, 1-5 min 10-50% B, 5-

13 min 50-90% B, 13-16 min 90% B and finally the column was reconditioned with 10% B for 2 min. The injection volume was 2 μL.

High resolution mass detection was achieved on a Q-Exactive-Orbitrap mass spectrometer (Thermo Fisher Scientific, USA) equipped with an ESI interface operated in positive ion mode. Source parameters were optimized as follows: spray voltage 3.0 kV, capillary temperature 300 ºC, sheath gas 40 arb, and auxiliary gas 10 arb. Mass scans were acquired in the *m/z* range of 100–1000 Da in centroid mode with a mass resolution of 70000 FWHM. MS/MS spectra were recorded with dd-MS^2 data acquisition mode with higher-energy collisional dissociation at 25 eV. Instrumental control and data acquisition were conducted by Xcalibur software (Version 2.3.1, Thermo Fisher Scientific, USA).

2.6. Method validation

2.6.1. Selectivity

To investigate the selectivity of the quantitation method, blank rat plasma from six different individuals, blank rat plasma spiked with GW9508 at lower limit of quantification (LLOQ) and IS, and actual rat plasma after oral administration of GW9508 were prepared and analyzed as above-mentioned procedures. There should be no interfering peaks at the retention times of GW9508 and IS.

2.6.2. Linearity and sensitivity

The calibration curves, ranging from 1 to 1000 ng/mL, were constructed by plotting the peak area ratio of GW9508 to IS (*y*) versus nominal concentration of GW9508 (*x*). The linearity was assessed by correlation coefficient (*r*), which should be > 0.995. The sensitivity was expressed as LLOQ, at which the signal-to-noise ratio was >10, with acceptable accuracy and precision.

2.6.3. Precision and accuracy

The intra- and inter-day precision and accuracy of the assay were investigated by analyzing sextuplicates of each concentration levels (3, 30 and 750 ng/mL) on three successive days along with a freshly prepared calibration curve each day. Precision was expressed as RSD% (relative standard deviation) of the QC samples, which should be < 15%, while accuracy was indicated as RE% (relative error), which should be within ±15%.

2.6.4. Extraction recovery and matrix effects

Extraction recovery and matrix effects were evaluated by QC samples at three concentration levels (3, 30 and 750 ng/mL). Extraction recovery of GW9508 was evaluated by comparing the peak areas of GW9508 from pre-extracted QC samples with those of samples reconstituted with blank extracted plasma (post-extraction) at the same concentrations. The matrix effects were evaluated with six different lots of rat plasma. Matrix effects were measured by comparing the peak areas of post-extraction blank plasma samples spiked with GW9508 with those of standard solutions at the same concentrations. The values of matrix effects (ME%) should be in the range of 85-115%. The extraction recovery and matrix effects of IS were determined in the same procedure.

2.6.5. Stability

The stability of GW9508 in rat plasma was assessed by QC samples at three concentration levels (3, 30 and 750 ng/mL) in sextuplicates under different storage conditions. Long-term stability was performed at -80 °C for 30 days; short-term stability was conducted at 25 °C for 12 h; post-preparative stability was carried out at 10 °C for 8 h in auto-sampler; and freeze-thaw stability was performed after three freeze (-80 °C)-thaw (25 °C) cycles. All the QC samples were measured by a freshly

prepared calibration curve. The determined concentrations should be within ± 15% of the nominal concentrations and RSD% should be < 15%.

2.6.6. Dilution integrity

The effect of dilution was evaluated by diluting six replicates of QC samples at a concentration 4 μg/mL with blank rat plasma to yield the final concentration of 1000 ng/mL. The diluted samples were processed and determined as above. The accuracy should be within ± 15% of the nominal concentration with RSD% < 15%.

3. Results and discussion

3.1. Method development

To accurately quantify GW9508 in rat plasma, the mass spectra of GW9508 and IS were initially obtained. Compared with that in negative ion mode, GW9508 showed much higher mass signal in positive ion mode. In full-mass scan, GW9508 and IS displayed protonated molecular ions [M+H]$^+$ at *m/z* 348.2 and 397.2, respectively. In product ion scan, GW9508 produced two abundant product ions at *m/z* 288.1 and 183.1; IS resulted in the product ions at *m/z* 260.2 and 138.0. Further experiments demonstrated that transition of *m/z* 348.2→183.1 was more sensitive than that of *m/z* 348.2→288.1; for IS, transitions of *m/z* 397.2→260.2 and *m/z* 397.2→138.0 showed the identical sensitivity. Therefore, the quantifier precursor-to-product transitions were *m/z* 348.2→183.1 for GW9508 and *m/z* 397.2→260.2 for IS. For confirmation, qualifier precursor-to-product transitions were *m/z* 348.2→288.1 and *m/z* 397.2→138.0 for GW9508 and IS, respectively. The source parameters, S-Lens voltage and collision energy were further optimized to obtain the optimum sensitivity.

ZORBAX Eclipse XDB C$_{18}$ column (50 mm × 2.1 mm, 5 μm) was selected for separation, which had a good separation performance, short running time and symmetric peak shape. Methanol and acetonitrile were compared, and acetonitrile with gradient elution had better elution ability, which guaranteed a thorough separation in such a short running time (2 min). Addition of 0.1% formic acid in the mobile was found to facilitate the ionization of the analyte and IS.

Protein precipitation with organic solvent was frequently used for sample preparation. In this study, acetonitrile was employed for plasma pretreatment. Unfortunately, leading peak was found when the supernatant was directly injected for analysis. To obtain a symmetric peak shape, the supernatant was dried to dryness and the residue was re-dissolved in 100 μL of acetonitrile-water solution (*v/v*; 1:9).

3.2. Method validation

3.2.1. Selectivity

Fig. 1 showed the representative SRM chromatograms of blank rat plasma, blank rat plasma supplemented with GW9508 and IS, and plasma samples after oral administration of GW9508. It was indicated that GW9508 was well separated and no interfering peak was found at the retention times of GW9508 and IS. Under the current conditions, GW9508 and IS were detected at 1.27 and 0.64 min, respectively.

3.2.2. Linearity and sensitivity

The calibration curves were linear in the range of 1-1000 ng/mL, with correlation coefficient larger than 0.998 ($r > 0.998$). The typical calibration curve is $y = 0.0062\, x + 0.0071$, where y is peak area ratio of GW9508/IS and x is the concentration of GW9508 in plasma (ng/mL). The sensitivity of this

assay indicated by LLOQ was 1 ng/mL, where the RE% ranged from -8.45% to 6.34% and the RSD% were less than 8.63%.

3.2.3. Precision and accuracy

As summarized in **Table 1**, the intra- and inter-day RSD% were less than 6.25% and 7.97%, respectively; intra- and inter-day RE% were in the range of -2.33-4.80% and -6.70-7.80%, respectively. These data suggested that GW9508 in rat plasma can be accurately and precisely measured by the developed assay.

3.2.4. Extraction recovery and matrix effects

As shown in **Table 1**, the extraction recovery of GW9508 from rat plasma was more than 84.34% and the extraction recovery of IS was 81.02%. The results of matrix effects suggested that the developed assay was free of matrix effects. ME% values were in the range of 93.51-103.74%.

3.2.5. Stability

GW9508 was stable in rat plasma at -80 ºC for 30 days, 25 ºC for 12 h, 10 ºC for 8 h in auto-sampler, and after three freeze (-80 ºC)-thaw (25 ºC) cycles. The RE% values ranged from -5.33% to 3.67% with RSD% < 8.01%.

3.2.6. Dilution integrity

The results of dilution integrity indicated that 4-fold dilution of the plasma sample did not significantly affect the determination of GW9508, with RE% in the range of -2.33-3.67% and RSD% of 3.83%.

3.3. Pharmacokinetic study

The validated LC/MS/MS has been successfully applied to the pharmacokinetics study of GW9508 in rat plasma. **Fig. 2** depicted the plasma concentration-time curves of GW9508 in rat plasma after

oral and intravenous administration at a single dose of 1 mg/kg. The primary pharmacokinetic parameters calculated through non-compartmental analysis using DAS 2.0 software (Chinese Pharmacology Society) were summarized in **Table 2.** After intravenous administration, GW9508 was slowly eliminated from the plasma, with half-life ($T_{1/2}$) of 7.34 h and clearance (CL) of 239.45 mL/h/kg. The exposure (AUC_{0-t}) was 3791.02 ng·h/mL. When given orally, GW9508 was rapidly absorbed into plasma as indicated by the evidence that GW9508 was detectable at 5 min post-dose, and reached the maximum plasma concentration (C_{max}) at 1.50 h post-dose. The CL was 482.43 mL/h/kg and the $T_{1/2}$ was 5.08 h. The oral bioavailability was calculated to be 54.88%. Taken together, after oral or intravenous administration, GW9508 showed low clearance, moderate elimination half-life, high exposure and ideal bioavailability.

3.4. Metabolism study

3.4.1. Mass fragmentation of GW9508

To obtain some structural information, mass fragmentation of GW9508 was initially investigated. In positive ion mode, GW9508 showed accurate protonated molecular ion $[M+H]^+$ at *m/z* 348.1578 (theo. *m/z* 348.1594) with chemical formula being $C_{22}H_{22}NO_3^+$. MS^2 fragmentation of this ion resulted in four characteristic fragment ions at *m/z* 330.1470 (theo. *m/z* 330.1489), 288.1375 (theo. *m/z* 288.1383), 183.0799 (theo. *m/z* 183.0804) and 178.0857 (theo. *m/z* 178.0863), as displayed in **Fig. 3**. The fragment ion at *m/z* 330.1470 was from the molecular ion $[M+H]^+$ through the loss of H_2O (-18.0108 Da). The fragment ion at *m/z* 288.1375 derived from the molecular ion $[M+H]^+$ by the loss of acetic acid (-60.0203 Da). The fragment ion at *m/z* 183.0799 was attributed to the *meta*-phenoxybenzyl, which was formed from molecular ion by the cleavage of *para*-aminophenylpropanoic acid (-

165.0779 Da). The fragment ion at *m/z* 178.0857 derived from the molecular ion by the loss of oxydibenzene moiety (-170.0721 Da).

3.4.2. Structural elucidation of the metabolites

Comparison of drug-containing samples with those of blank controls resulted in the identification of seven metabolites. The MDF chromatograms of the metabolites and parent from rat plasma, rat hepatocytes and human hepatocytes were displayed in **Fig. 4.** In rat plasma and hepatocytes, three metabolites (M1, M4 and M6) were detected, while seven metabolites were found in human hepatocytes. M2, M3, M5 and M7 were human specific. These metabolites could be classified into three types, i. e., hydroxylation, hydroxylation with glucuronidation, and glucuronidation. The retention time, measured *m/z*, theoretical *m/z* and fragment ions of each metabolite were summarized in **Table 3.**

Metabolites M1 and M2: M1 and M2 were separated at the retention times of 5.33 and 5.63 min, respectively. They had the same protonated molecular ion [M+H]$^+$ at *m/z* 540.1857 (mass error -1.3 ppm), with chemical formula being $C_{28}H_{30}NO_{10}^+$, suggesting that M1 and M2 were hydroxylation with glucuronidation of parent. MS^2 fragmentation **(Fig. 5)** of this ion resulted in a diagnostic fragment ion at *m/z* 364.1533, which derived from precursor ion by the loss of glucuronyl (-176.0324 Da). This fragmentation is a typical neutral loss of glucuronide conjugate. Another characteristic fragment ion at *m/z* 199.0751 indicated that hydroxylation occurred at *meta*-phenoxybenzyl moiety. The other fragment ions at *m/z* 346.1436, 304.1325 and 178.0859 were identical to those of parent.

Metabolites M3, M4 and M5: M3, M4 and M5 were detected at the retention times of 5.65, 6.54 and 6.66 min, respectively. In full-mass scan, they shared the identical protonated molecular ion

[M+H]$^+$ at *m/z* 364.1532 (mass error -3.0 ppm), 15.9938 Da larger than that of parent, suggesting the presence of hydroxyl group in the molecules. MS^2 fragmentation of this ion yielded four fragment ions at *m/z* 346.1430, 304.1326, 199.0750, and 178.0859, as shown in **Fig. 6**. The fragment ion at *m/z* 199.0750 was 15.9946 Da larger than that of parent (*m/z* 183.0804), suggesting that hydroxylation occurred at *meta*-phenoxybenzyl moiety. The other fragment ions were identical to those of parent.

Metabolite M6: M6 was separated at 7.10 min, with a protonated molecular ion [M+H]$^+$ at *m/z* 524.1907 (mass error -1.5 ppm, chemical formula $C_{28}H_{30}NO_9^+$), 176.0313 Da higher than that of parent, suggesting that M6 was the glucuronide conjugate of parent. MS^2 fragmentation of this ion **(Fig. 7)** resulted in a fragment ion at *m/z* 348.1586, which resulted from precursor ion by the loss of glucuronyl (-176.0313 Da). This fragmentation is a typical neutral loss of glucuronide conjugate. The other fragment ions at *m/z* 330.1480, 288.1375 and 183.0798 were identical to those of parent.

Metabolite M7: M7 was detected at 7.12 min, with a protonated molecular ion [M+H]$^+$ at *m/z* 364.1532 (mass error -3.0 ppm, chemical formula $C_{22}H_{22}NO_4^+$), 15.9938 Da higher than that of parent, suggesting the presence of hydroxyl group in the molecule. MS^2 fragmentation **(Fig. 8)** of this ion resulted in a fragment ion at *m/z* 183.0801, which was identical to that of parent, suggesting the unmodification of *meta*-phenoxybenzyl moiety. The other fragment ions at *m/z* 346.1428, 304.1323 and 194.0801 were 16 Da higher than those of parent, demonstrating the occurrence of hydroxylation at *para*-aminobenzyl moiety.

3.4.3. Metabolic pathways

Based on the identified metabolites, the metabolic pathways of GW9508 were proposed, as shown in **Fig. 9.** The metabolic pathways of GW9508 could be mainly concluded as hydroxylation and

glucuronidation. M6 (acylglucuronide conjugate) was the most abundant metabolite in all tested matrices. As acylglucuronide is reactive in some cases, and is responsible for some liver injury. Therefore, the next works will focus on the safety assessment of this metabolite.

4. Conclusions

In conclusion, a simple and reliable LC/MS/MS method combined with protein precipitation procedure was developed and validated for the determination of GW9508 in rat plasma. The total running time was 2 min and the LLOQ was 1 ng/mL. The newly proposed method has been employed to explore the pharmacokinetic profile of GW9508 in rat plasma. Our results revealed that GW9508 showed low clearance, moderate half-life and excellent bioavailability (54.88%). Furthermore, an LC-Q-Exactive-Orbitrap-MS was developed to detect and identify the metabolites of GW9508 present in rat plasma, rat hepatocytes and human hepatocytes. A total of seven metabolites were detected and structurally characterized. Hydroxylation and glucuronidation were demonstrated to be the primary metabolic pathways.

References

[1] R. A. Defronzo, Banting Lecture. From the triumvirate to the ominous octet: a new paradigm for the treatment of type 2 diabetes mellitus, Diabetes **58** (2009) 773-795

[2] G. Danaei, M. M. Finucane, Y. Lu, et al. National, regional, and global trends in fasting plasma glucose and diabetes prevalence since 1980: systematic analysis of health examination surveys and epidemiological studies with 370 country-years and 2.7 million participants, Lancet **378** (2011) 32-40

[3] O. J. Phung, J. M. Scholle, M. Talwar, C. I. Coleman. Effect of noninsulin antidiabetic drugs added to metformin therapy on glycemic control, weight gain, and hypoglycemia in type 2

diabetes, JAMA **303** (2010) 1410–1418

[4] M. A. Avery, C. S. Mizuno, A. G. Chittiboyina, T. W. Kurtz, H. A. Pershadsingh, Type 2 diabetes and oral antihyperglycemic drugs, Curr. Med. Chem. **15** (2008) 61–74

[5] B. L. Wajchenberg, beta-cell failure in diabetes and preservation by clinical treatment, Endocr. Rev. **28** (2007) 187-218

[6] Y. Itoh, Y. Kawamata, M. Harada, M. Kobayashi, R. Fujii , S. Fukusumi, K. Ogi, M. Hosoya, Y. Tanaka, H. Uejima, H. Tanaka, M. Maruyama, R. Satoh, S. Okubo, H. Kizawa, H. Komatsu, F. Matsumura, Y. Noguchi, T. Shinohara, S. Hinuma, Y. Fujisawa, M. Fujino, Free fatty acids regulate insulin secretion from pancreatic β cells through GPR40, Nature **422** (2003) 173–176

[7] E. Flodgren, B. Olde, S. Meidute-Abaraviciene, M. S. Winzell, B. Ahrén, A. Salehi, GPR40 is expressed in glucagon producing cells and affects glucagon secretion, Biochem. Biophys Res. Commun. **354** (2007) 240–245

[8] Z. Li, Q. Q. Qiu, X. Q. Geng, J. Y. Yang, W. L. Huang, H. Qian, Free fatty acid receptor agonists for the treatment of type 2 diabetes: drugs in preclinical to phase II clinical development, Expert Opin. Inv. Drug **25** (2016) 871-890

[9] I. G. Tikhonova, C. S. Sum, S. Neumann, S. EWngel, B. M. Rkkaa, S. Costanzi, M. C. Gershengorn, Discovery of novel agonists and antagonists of the free fatty acid receptor 1 (FFAR1) using virtual screening, J. Med. Chem. **51** (2018) 625–633

[10] Z. Li, Q. Q. Qiu, X. Q. Geng, J. Y. Yang, W. L. Huang, H. Qian, Free fatty acid receptor agonists for the treatment of type 2 diabetes: drugs in preclinical to phase II clinical development, Expert Opin. Inv. Drug **25** (2016) 871–890

[11] S. C. McKeown, D. F. Corbett, A. S. Goetz, T. R. Littleton, E.W. Biogham, C. P. Briscoe, A.J.

Peat, S. P. Watson, D. M. Hickey, Solid phase synthesis and SAR of small molecule agonists for the GPR40 receptor, Bioorg. Med. Chem. Lett. **17** (2007) 1584–1589

[12] J. B. House, L. Zhu, Y. Sun, M. Akerman, W. Qiu, A.J. Zhang, R. Sharma, M. Schmitt, Y. Wang, J. Liu, J. C. Medina, J. D. Reagan, J. Luo, G. Tonn, J. Zhang, J. Y. Lu, M. Chen, E. Lopez, K. Nguyen, L. Yang, L. Tang, H. Tian, S. J. Shuttleworth, D. C. Lin, AMG 837: a potent, orally bioavailable GPR40 agonist, Bioorg Med Chem Lett. **22** (2012) 1267–1270

[13] S. Mikami, S. Kitamura, N. Negoro, S. Sasaki, M. Suzuki, Y. Tsujihata, T. Miyazaki, R. Ito, N. Suzuki, J. Miyazaki, T. Santou, N. Kanzaki, M. Funami, T. Tanaka, T. Yasuma, Y. Momose, Discovery of phenylpropanoic acid derivatives containing polar functionalities as potent and orally bioavailable G protein-coupled receptor 40 agonists for the treatment of type 2 diabetes, J. Med. Chem. **55** (2012) 3756–3776

[14] Z. Li, X. Xu, W. L. Huang, H. Qian, Free Fatty Acid Receptor 1 (FFAR1) as an Emerging Therapeutic Target for Type 2 Diabetes Mellitus: Recent Progress and Prevailing Challenges, Med. Res. Rev. **38** (2018) 381-425

[15] K. Kaku, T. Araki, R. Yoshinaka, Randomized, double-blind, dose-ranging study of TAK-875, a novel GPR40 agonist, in Japanese patients with inadequately controlled type 2 diabetes, Diabetes Care **36** (2013) 245-250

[16] M. S. Hedrington, S. N. Davis, Discontinued in 2013: diabetic drugs, Expert Opin. Inv. Drug, **23** (2014) 1703–1711

[17] D. M. Garrido, D. F. Corbett, K. A. Dwornik, A. S. Goetz, T. R. Littleton, S. C. McKeown, W. Y. Mills, T. L. Smalley Jr, C. P. Briscoe, A. J. Peat, Synthesis and activity of small molecule GPR40 agonists, Bioorg. Med. Chem. Lett. **16** (2006) 1840-1845

[18] C. P. Briscoe, A. J. Peat, S. C. McKeown, D. F. Corbett, A. S. Goetz, T. R. Littleton, D. C. McCoy, T. P. Kenakin, J. L. Andrews, C. Ammala, J. A. Fornwald, D. M. Ignar, S. Jenkinson, Pharmacological regulation of insulin secretion in MIN6 cells through the fatty acid receptor GPR40: identification of agonist and antagonist small molecules, Br. J. Pharmacol. **148** (2006) 619-28

[19] H. Y. Ou, H. T. Wu, H. C. Hung, Y. C. Yang, J. S. Wu, C. J. Chang, Multiple mechanisms of GW-9508, a selective G protein-coupled receptor 40 agonist, in the regulation of glucose homeostasis and insulin sensitivity, Am. J. Physiol-Endocr. Metab. **304** (2013) 668-676

[20] D. M. Garrido, D. F. Corbett, K. A. Dwornik, A. S. Goetz, T. R. Littleton, S. C. McKeown, W. Y. Mills, T. L. Smalley Jr, C. P. Briscoe, A. J. Peat, Synthesis and activity of small molecule GPR40 agonists, Bioorg. Med. Chem. Lett. **16** (2006) 1840-1845

[21] Y. F. Zhao, L. Wang, D. Zha , L. Qiao, L. Lu, J. Yu, P. Qu, Q. Sun, J. Qiu, C. Chen, GW9508 inhibits insulin secretion by activating ATP-sensitive potassium channels in rat pancreatic β-cells, J. Mol. Endocrinol. **51** (2013) 69-77

[22] C. Y. He, H. Wan, Drug metabolism and metabolite safety assessment in drug discovery and development, Expert Opin. Drug Metab. Toxicol. **14** (2018) 1071-1085

[23] S. C. McKeown, D. F. Corbett, A. S. Goetz, T. R. Littleton, E. Bigham, C. P. Briscoe, A. J. Peat, S. P. Watson, D. M. Hickey, Solid phase synthesis and SAR of small molecule agonists for the GPR40 receptor, Bioorg. Med. Chem. Lett. **17** (2007) 1584-1589

[24] H. Y. Zhang, D. L. Zhang, K. Ray, M. S. Zhu, Mass defect filter technique and its applications to drug metabolite identification by high-resolution mass spectrometry, J. Mass. Spectrom. **44** (2009) 999-1016

[25] R. A. Hamilton, W. R. Garnett, B.J. Kline, Determination of mean valproic acid serum level by assay of a single pooled sample, Clin. Phurmacol. Ther. **29** (1981) 408-413

[26] C. E. Hop, Z. Wang, Q. Chen, G. Kwei, Plasma-Pooling Methods To Increase Throughput for *in vivo* Pharmacokinetic Screening, J. Pharm. Sci. **87** (1998) 901-903

Figure legends

Fig. 1. SRM chromatograms of **(A)** blank rat plasma, **(B)** blank rat plasma spiked with GW9508 at LLOQ and IS, and **(C)** rat plasma after oral administration of GW9508. GW9508 and IS were detected at 1.27 and 0.64 min, respectively.

(A)

IS: *m/z* 397.2→260.2

GW9508: *m/z* 348.2→183.1

(B)

IS: *m/z* 397.2→260.2

GW9508: *m/z* 348.2→183.1

(C)

IS: *m/z* 397.2→260.2

GW9508: *m/z* 348.2→183.1
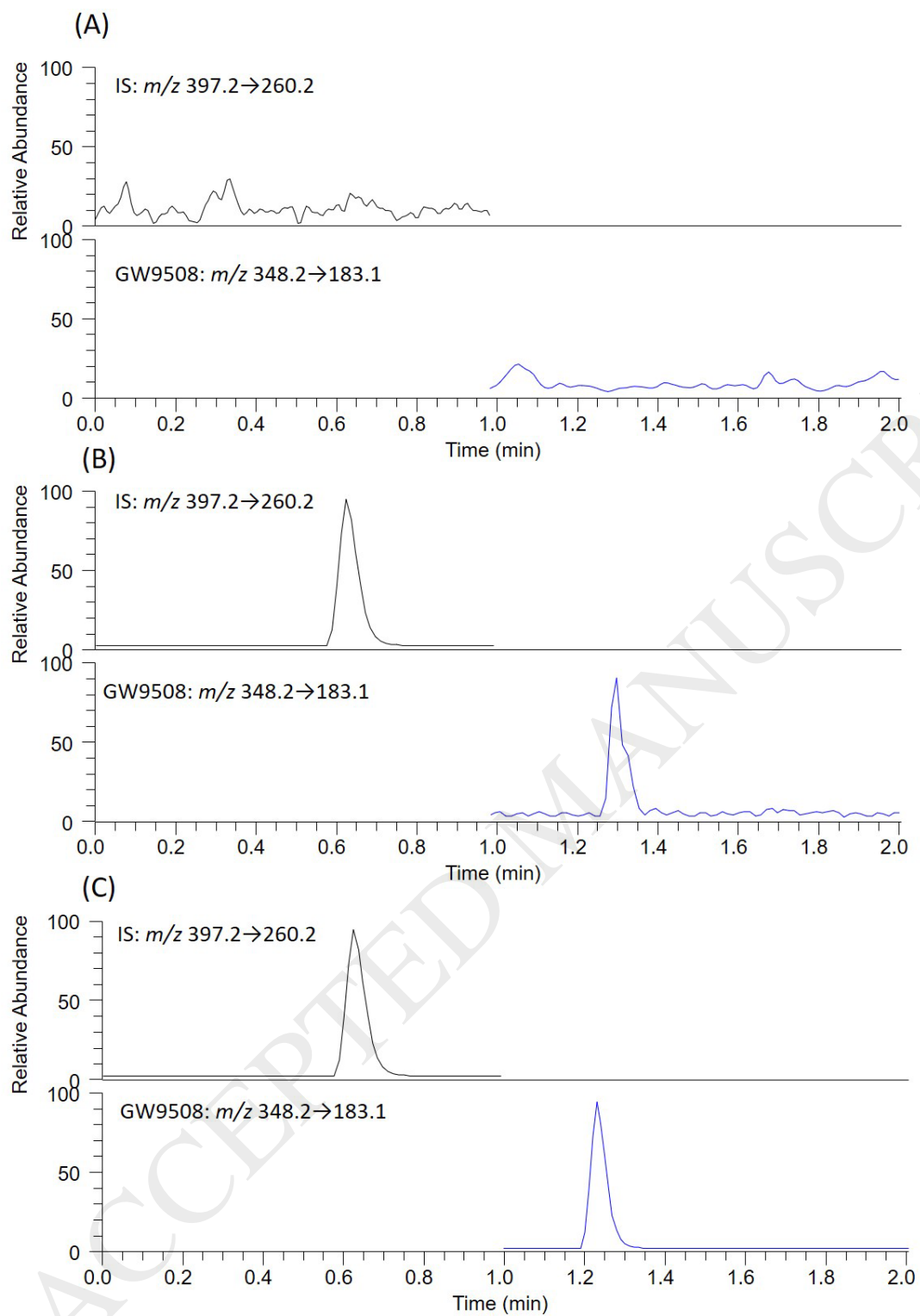
Fig. 2. Plasma concentration (ng/mL) versus time (h) curves of GW9508 after oral and intravenous

administration of GW9508 at a single dose of 1 mg/kg ($n = 6$)
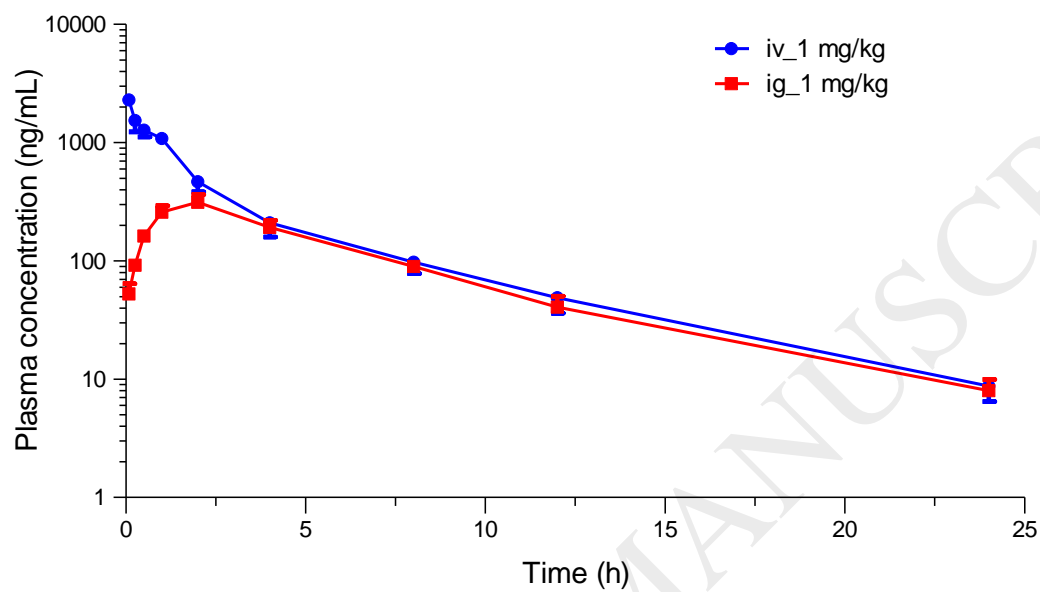
Fig. 3. MS^2 spectrum of GW9508 and its fragmentation pathways

F: FTMS + c ESI d Full ms2 348.16@hcd17.33 [50.00-375.00]

(a)

(b)

GW9508, *m/z* 348.1578
(Theo. *m/z* 348.1594)

m/z 288.1375
(Theo. *m/z* 288.1383)

m/z 183.0799
(Theo. *m/z* 183.0804)

m/z 330.1470
(Theo. *m/z* 330.1489)

m/z 178.0857
(Theo. *m/z* 178.0863)
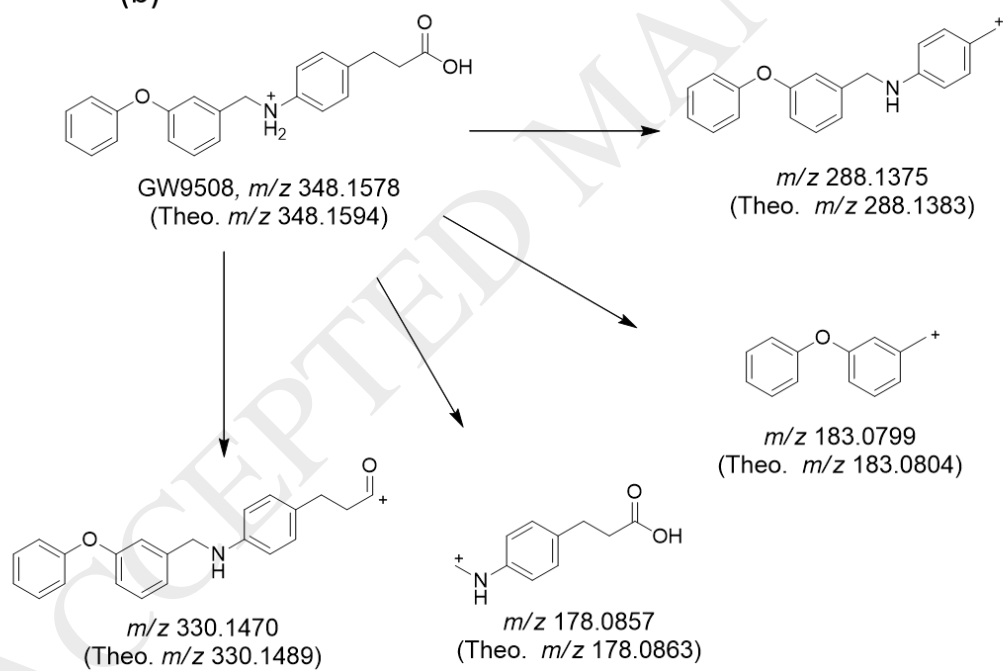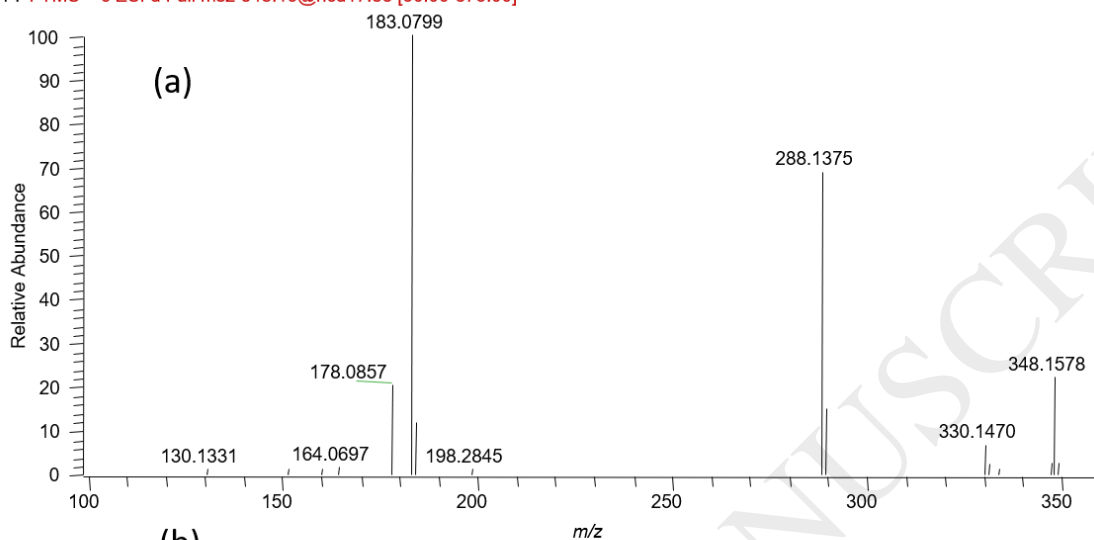
Fig. 4. MDF (mass defect filter) chromatograms of GW9508 and its metabolites from rat plasma, rat hepatocytes and human hepatocytes.
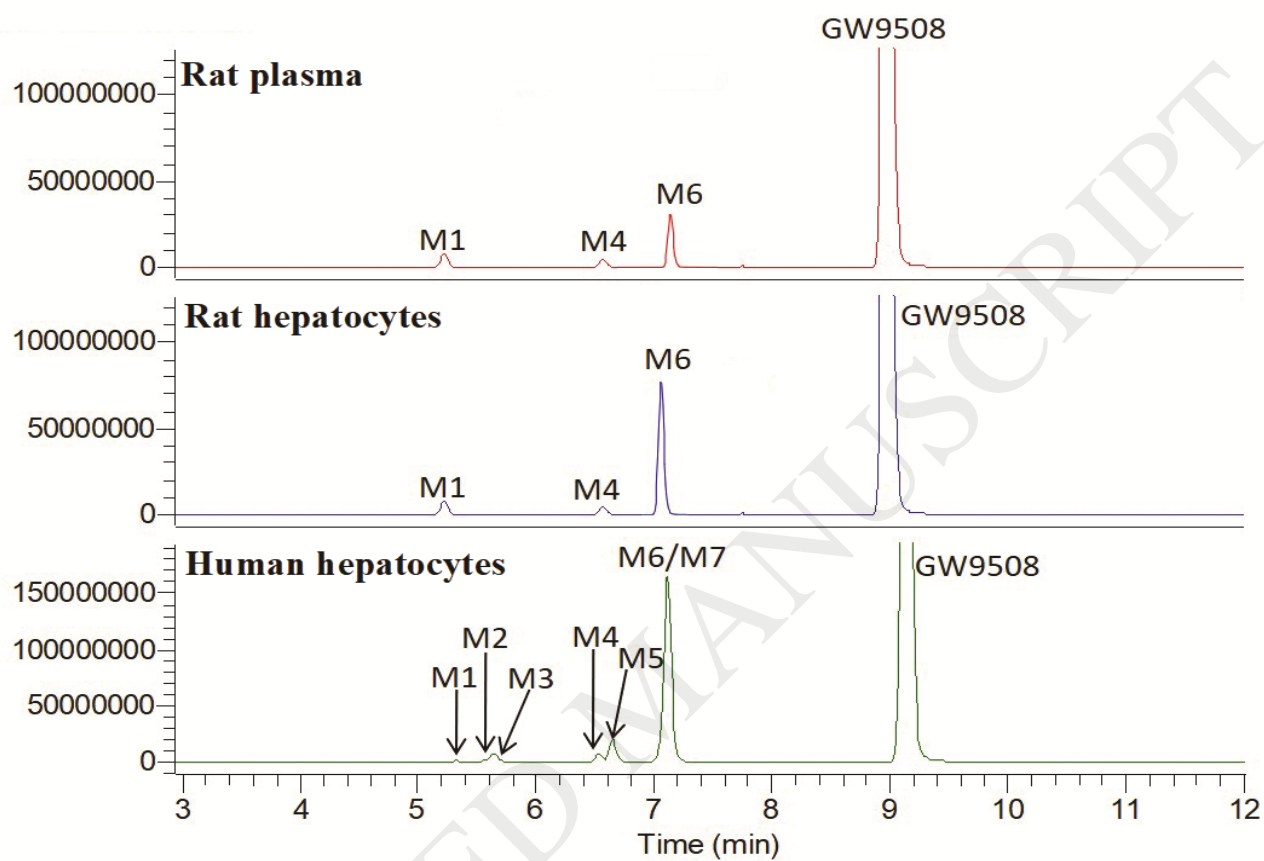
Fig. 5. MS^2 spectrum of M1 and M2 along with the fragmentations
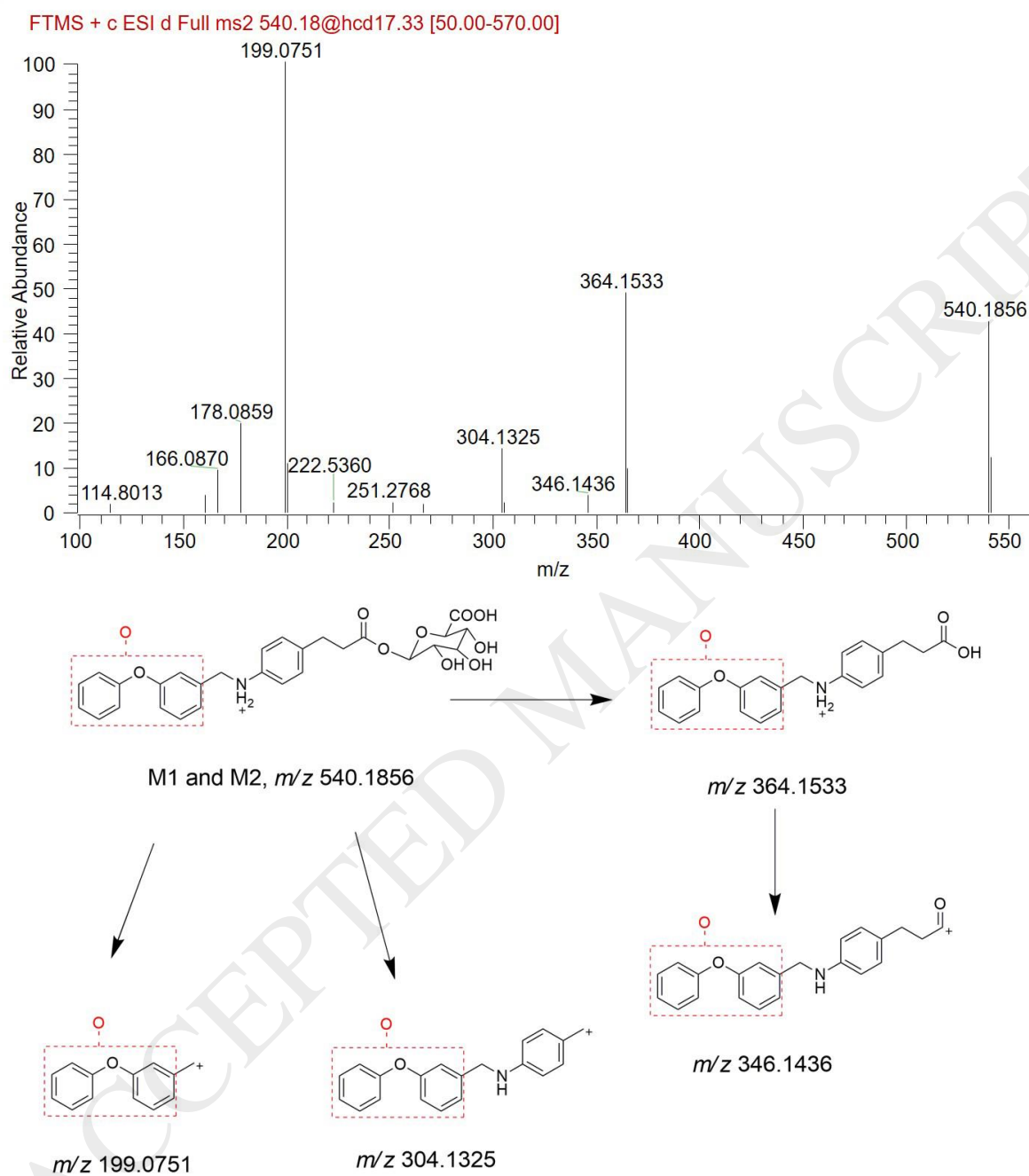
Fig. 6. MS^2 spectrum of M3, M4 and M5 along with the fragmentations
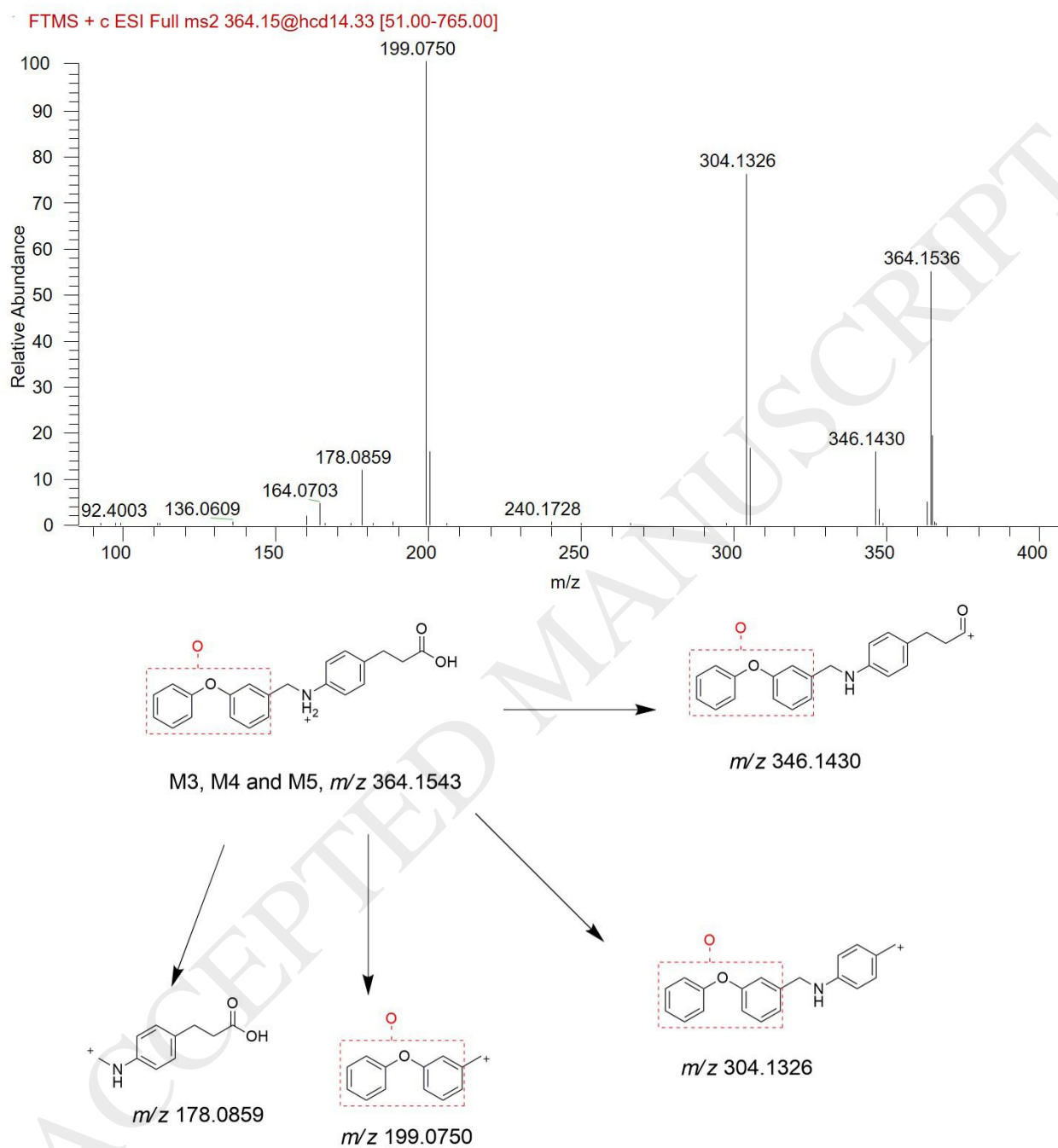
Fig. 7. MS^2 spectrum of M6 along with the fragmentations

FTMS + c ESI Full ms2 524.19@hcd14.33 [72.67-1090.00]
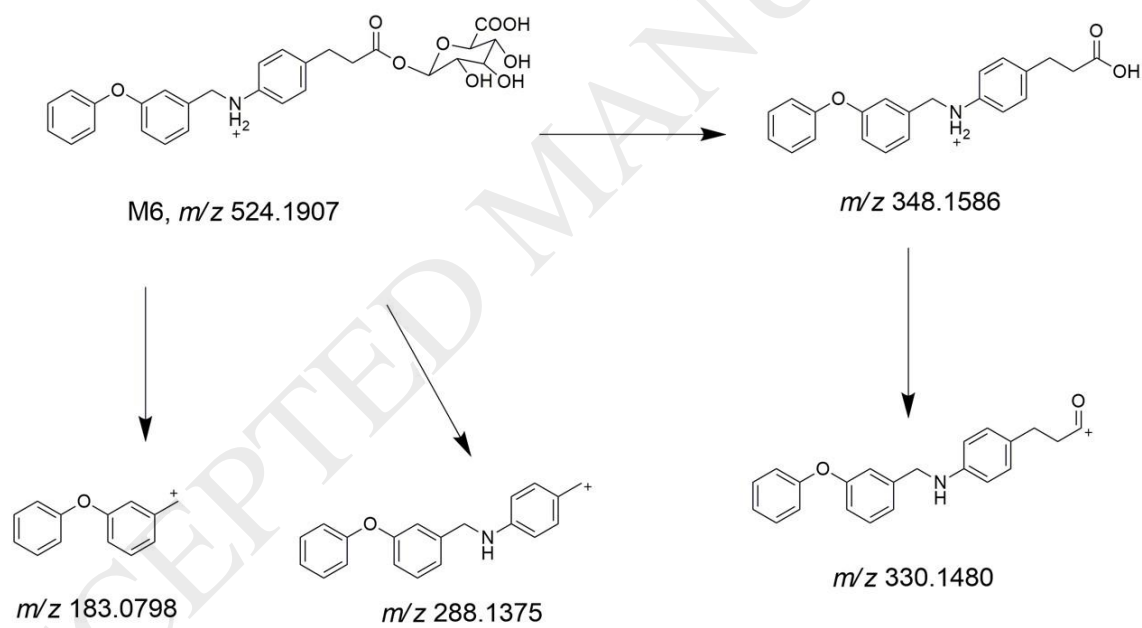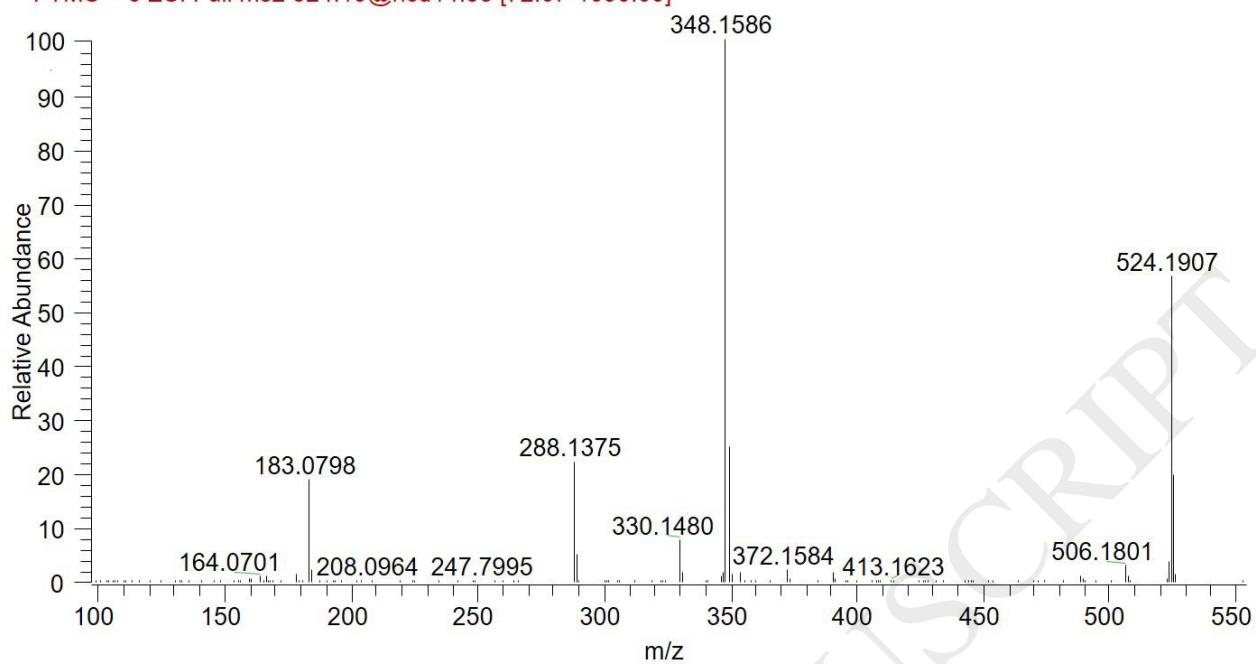
Fig. 8. MS^2 spectrum of M7 along with the fragmentations

FTMS + c ESI Full ms2 364.15@hcd14.33 [51.00-765.00]
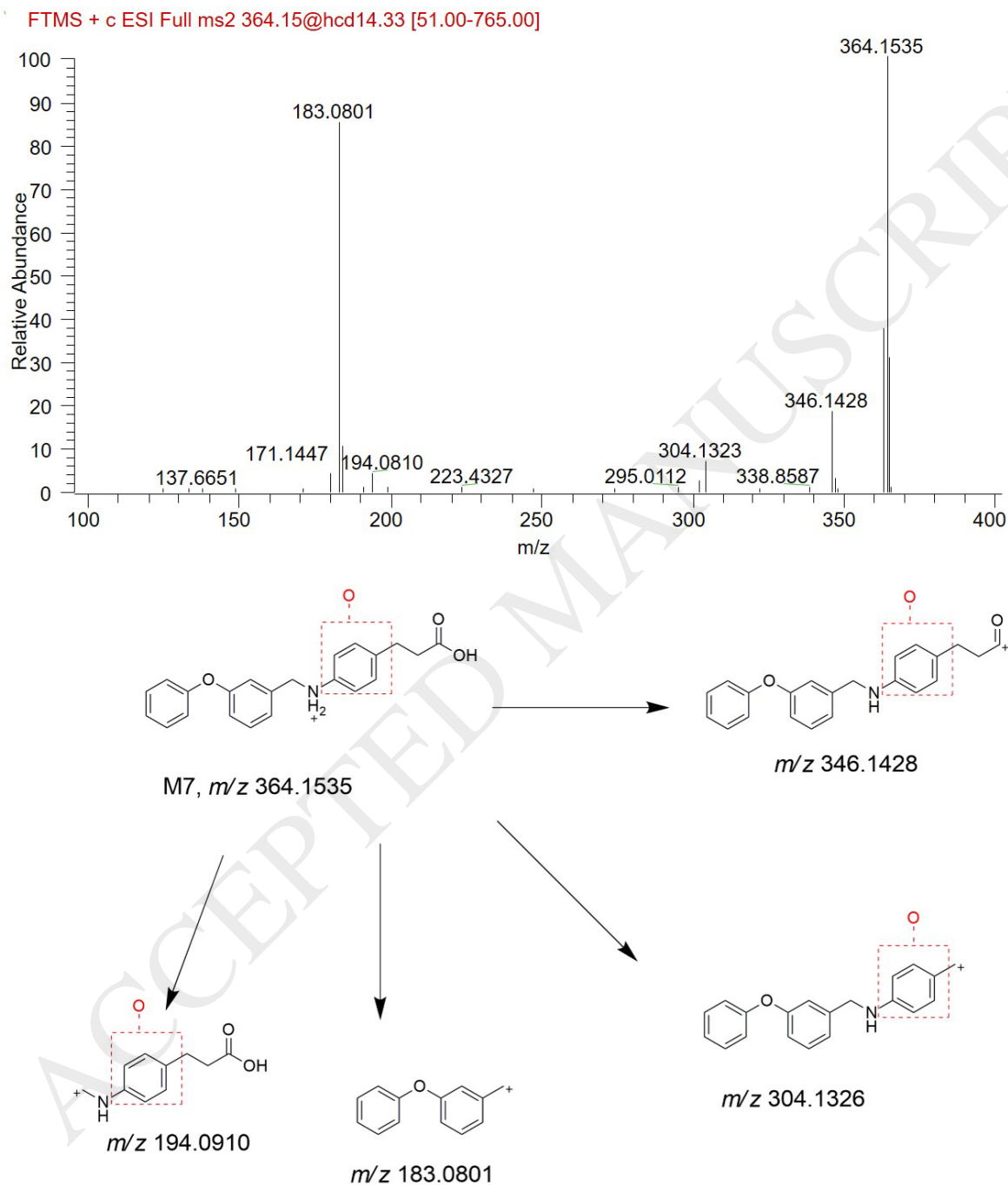
Fig. 9. Proposed metabolic pathways of GW9508 in rat plasma, rat hepatocytes and human hepatocytes

GW9508, MW = 347

Hydroxylation

M7 (H), MW = 363

Hydroxylation

Glucuronidation

M3 (H), M4 (R, H), M5 (H), MW = 363

M6 (R, H), MW = 523

Glucuronidation

M1 (R, H), M2 (H), MW = 539
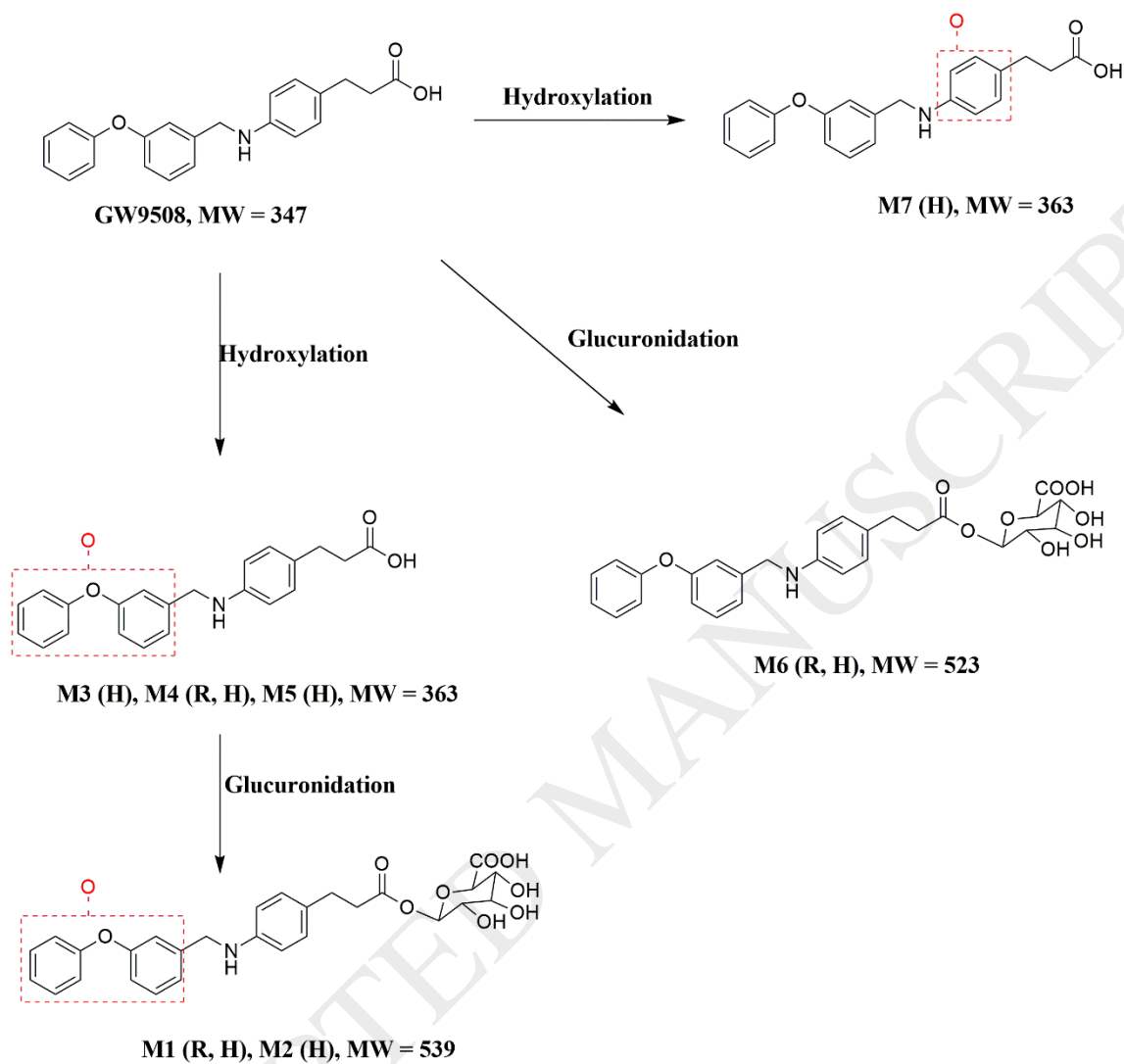
R and H represent rat and human, respectively

Table 1. Precision, accuracy, matrix effects and extraction recovery of GW9508 ($n = 6$)

Analyte	Spiked Concentration (ng/mL)	Intra-day		Inter-day		Matrix effects (%)	Extraction recovery (%)
		Precision (RSD%)	Accuracy (RE%)	Precision (RSD%)	Accuracy (RE%)		
	3	3.08	-2.33	4.41	-6.7	103.74 ± 3.65	86.83 ± 4.32
GW9508	30	6.25	3.60	7.09	7.80	98.45 ± 9.41	84.34 ± 5.89
	750	1.59	4.80	7.97	1.73	93.51 ± 4.55	83.90 ± 6.91
IS	40					96.95 ± 8.21	81.02 ± 3.21

Table 2. Pharmacokinetic parameters of GW9508 in rat plasma after oral and intravenous administration at a single dose of 1 mg/kg

Parameters	Intravenous ($n = 6$)	Oral ($n = 6$)
AUC_{0-t} (ng·h/mL)	3791.02 ± 444.38	2021.53 ± 213.64
AUC_{0-inf} (ng·h/mL)	3806.34 ± 452.44	2088.95 ± 217.41
MRT_{0-t} (h)	4.44 ± 0.65	5.57 ± 0.84
MRT_{0-inf} (h)	4.68 ± 0.58	6.42 ± 1.19
$T_{1/2}$ (h)	7.34 ± 1.33	5.08 ± 1.65
C_{max} (ng/mL)	2292.25 ± 876.03	364.25 ± 69.58
T_{max} (h)		1.50 ± 0.58
CL (mL/h/kg)	239.45 ± 57.30	482.43 ± 48.32
Vd (mL/kg)	2551.14 ± 791.07	3427.07 ± 1003.77

F%   54.88

AUC, area under the curve; MRT, mean resident time; T1/2, half-life; C_{max}, maximum plasma concentration; T_{max}, time to reach C_{max}; CL, clearance; Vd, volume of distribution. The bioavailability (F%) was calculated as $(AUC_{0\text{-inf, oral}})/(AUC_{0\text{-inf, intravenous}}) \times 100\%$

Table 3. Metabolites of GW9508 present in rat plasma, rat hepatocytes and human hepatocytes

Met No.	RT (min)	Formula Change	Mass shift	Meas. m/z	Theo. m/z	Error (ppm)	Fragment ions	Identification	Source
M1	5.33	$[M + O + C_6H_8O_6]$	192.0263	540.1857	540.1864	-1.3	364.1533, 346.1436, 304.1325, 199.0751, 178.0859	Hydroxylation and glucuronidation	R, H
M2	5.63	$[M + O + C_6H_8O_6]$	192.0263	540.1857	540.1864	-1.3	364.1533, 346.1436, 304.1325, 199.0751, 178.0859	Hydroxylation and glucuronidation	H
M3	5.65	$[M + O]$	15.9938	364.1532	364.1543	-3.0	346.1430, 304.1326, 199.0750, 178.0859	Hydroxylation	H
M4	6.54	$[M + O]$	15.9938	364.1532	364.1543	-3.0	346.1430, 304.1326, 199.0750, 178.0859	Hydroxylation	R,H
M5	6.66	$[M + O]$	15.9939	364.1533	364.1543	-2.7	346.1430, 304.1326, 199.0750, 178.0859	Hydroxylation	H
M6	7.10	$[M + C_6H_8O_6]$	176.0313	524.1907	524.1915	-1.5	348.1586, 330.1480, 288.1375, 183.0798	Glucuronidation	R, H
M7	7.12	$[M + O]$	15.9938	364.1532	364.1543	-3.0	346.1428, 304.1323, 194.0801, 183.0801	Hydroxylation	H
GW9508	8.99	-	0.0000	348.1594	348.1582	3.4	330.1470, 288.1375, 183.0804, 178.0857	Parent	R, H